RED WoLF Hybrid Storage System: Comparison of CO_2 and Price targets

Alexander Alexandrovich Shukhobodskiy[1*], Aleksandr Zaitcev[1], Tatiana Pogarskaia[2], Giuseppe Colantuono[1**],

[1] *School of Built Environment, Engineering and Computing, Leeds Beckett University, Leeds, UK, LS1 3HE*

[2], *Institute of Applied Mathematics and Mechanics, Peter the Great St.Petersburg Polytechnic University, St.Petersburg, Russia*

Abstract

Innovative control method is prosed for the RED WoLF hybrid storage system. The technology is aimed for residential dwellings and allows to reduce the load from the electrical grid during time with high CO_2 emissions. The RED WoLF system consists of a battery, water cylinder, PV array and storage heaters. This technology allows the grid energy to be stored at the "greenest" time, in order to accommodate needs of dwellings with the aid of AI. The original RED WoLF algorithm is considerably improved, following modified progressive threshold approach up to additional 14% savings of CO_2 could be obtained. Intriguingly, savings are only slightly lower than global possible mathematical minimum, for the system barred of predictions errors. However, the computation time of the proposed control method is lower by a few orders of magnitudes, with comparison to standard optimisation techniques. Furthermore, the investigation on 11 months period was performed in order find out if there is significant difference between following a time of use tariff or an environmental signal. Results, suggest that the differences are minor in both cases following any signal improves the used energy quality. Although, the price signal has been affected slightly more to the choice of a target. Finally, the average system composition with 2 kWh battery and 4 kW PV array provides reduction by 55%-60% of both CO_2 emissions and the bill. Such achievement could potentially lead to smooth substitution of carbon intensive residential systems with gas and oil heaters.

Keywords: Hybrid Energy Storage, Photovoltaic, Artificial Intelligence, Peak Demand, Grid Integration

1. Introduction

Renewable energy generation propagates smoothly to the Power Grid, where storage has always been necessary to complement power plants with low flexibility. Historically, storage has been mainly positioned on the Grid side (e.g. pumped hydro) and combined with load following and peak plants. After deindustrialisation, it turned out to be useful in the British Isles and Australia to include thermal storage on the residential side (storage heaters), a simple technical solution to replace factories in generating a night time demand to accommodate inflexible coal power plants' output.

The cost of batteries has been continuously declining but still is high, and the high consumption of space heating in northern climates, where AC demand is on the other hand very low, made thermal storage (a blend of storage heaters and DHW (Domestic Hot Water) cylinders) the most straightforward and economical solution to combine heat storage and domestic heating electrification. The rise of renewables' share on the Grid, as well as the dwelling side, behind-the-meter PV generation (PV microgeneration from now on), provide a new, "modern" meaning and purpose to home energy storage. Fuel power plants have become more flexible and increased overall efficiency. However, flexible, fossil-fuel load-following plants usually work on a single cycle rather than on the combined cycle larger plants are based upon, which may result in the efficiency being roughly halved. This in turn, increases energy price and GHG (Green House Gases) emission. This would have an impact even in futuristic, renewable-only scenarios, with thermal plants used in combination with either biofuel, or CCS (Carbon Capture and Sequestration), or both, due to the higher amount of fuel/resources required.

The lack of frequency regulation capability of solar and wind plants makes storage necessary beyond simple energy balance. Combining thermal storage with battery and behind-the-meter PV generation, driven by AI algorithms based on forecasts of consumption, PV generation and Grid conditions may help the above-mentioned repurposing of home energy storage for the renewables era. The Interreg NWE RED WoLF project implements such a combination.

The reduction of CO_2 emissions is a challenge that faces whole World, as well it is a policy target of the European Union (EU). In order to achieve it, it is necessary to decarbonise the built environment, since it is a sector of the global economy that has one of the highest CO_2 emissions,

*Corresponding author, a.shukhobodskiy@leedsbeckett.ac.uk

**Corresponding author, g.colantuono@leedsbeckett.ac.uk

by increasing the percentage of renewable sources in the energy mix. Nevertheless, another crucial aim of the EU policy and mankind as a whole, is to fight fuel poverty, as indicated in innovation funding programs (Interreg NWE., 2019).

1.1. State-of-the-art

Hardware components of the RED WoLF system have been comprehensively analysed in many scientific reports. Battery storage technologies were analysed comprehensively by (Sufyan et al., 2019; Arani et al., 2019). Yan and Yang (2019) summarise the development of thermal storage published between 2009 and 2017. With 5 articles focused on peak-load shifting and 20 on more general topics of thermal storage within buildings. Felten and Weber (2018) suggest that the smart combination of heat pump and thermal storage can produce financial benefits. Another configuration was presented by Baeten et al. (2017), where heat pump with a hot water tank dedicated to space heating are joined together. It should be noted that thermodynamic work performed by the heat pump, requires power on demand in contrast to SHs.

Strategies to improve PV self consumption were addressed by Luthander et al. (2015). McKenna et al. (2013) test the performance of peak demand shifting by introducing batteries, where the same goal was pursued by managing appliances within a system Widén (2014). Later, comprehensive analysis including battery ageing and management was considered by (Hernndez et al., 2019, 2020; Gomez-Gonzalez et al., 2020; Muoz-Rodrguez et al., 2021).

Finally, HSS emerge by coupling PV array with heat pumps combined with thermal storage and batteries as presented by Kuboth et al. (2019) or Baniasadi et al. (2020) could lead to reduction of the operation cost. HSSs and the RED WoLF are geared toward future scenarios featuring abundant renewables but periodic energy supplies, where the time of energy uptake is of higher significance in comparison with the magnitude of energy generated. These possibilities found paramount consideration during recent time, especially when energy's wholesale reaches negative pricing (Ederer, 2015), wind energy demand and possible generation mismatch (Zhang et al., 2016; Andoni et al., 2017; Le et al., 2020), and solar energy is produced outside of demand periods, which is what leads, e.g., to the *duck curve* (Mills and Wiser, 2015; Hou et al., 2019).

Environmental impact of the various power management systems has also been thoroughly investigated in many recent works. Various potential scenarios to reduce CO_2 emissions were considered by comprehensive reviews of (Wagh and Kulkarni, 2018; Mohamad et al., 2018; Mohamad and Teh, 2018; Grosspietsch et al., 2019). Furthemore, the posibility of reducing "dirty" electrical intake for the Grid, for Battery and thermal storage Reda and Fatima (2019). The demand management on top of the storage system could lead to further energy savings as was recommended by Uddin et al. (2018). Then, Shukhobodskiy and Colantuono (2020) showed that combination of SHs, PV array, water cylinder and batteries has the potential to achieve the same goal, without a wet heating system being present. Afterwards, Ortiz et al. (2021) confirmed that the original progressive threshold approach can work even in the absence of thermal storage. Wiesheu et al. (2021) adapted the algorithm for countries with lower power intake. In addition to storage technologies and management systems, improvements in dynamic thermal rating could enhance the quality of electricity used within multiple dwelling (Teh and Lai, 2019; Metwaly and Teh, 2020).

1.2. Novelty

The main contribution of the manuscript is the advancement of the progressive thresholds approach control method. This method is compared to a standard optimisation technique in order to show the benefits of the proposed approach. Then the method is tested in a similation, where a Time-Of-Use Tariff (TOUT) is used alongside the CO_2 prediction from Shukhobodskiy and Colantuono (2020) in the governing algorithm. Like the forecast of CO_2 intensity index EI, the TOUT is assumed to be released with a 48 hours advance and half-hourly resolution; this actually occurs in Great Britain with the Octopus Energy "Agile Tariff" Ocotpus Energy (2020) employed in the simulations here reported. The difference is that, unlike the dynamically updated EI, TOUT is not being updated during the 48 hour interval, at the end of which a further 2 days tariff is released. Forecasts of PV generation and household consumption are still dynamically updated as in (Shukhobodskiy and Colantuono, 2020). Results in energy consumption, electricity bills and carbon emissions obtained by following the above mentioned EI and TOUT across 11 months period are reported, discussed and compared.

2. System design and algorithm

2.1. System design

In order to reduce price or CO_2 emissions we employ RED WoLF HSS Shukhobodskiy and Colantuono (2020). Such system consists of a battery, DHW cylinder, SHs and PV array Figure 1 presents symbolic representation of the HSS and control principles of RED WoLF system implemented in 100 pilot dwellings across the UK, Republic of Ireland and France. DHW cylinder, battery and SHs are all metered and are controlled by wireless switches directly through the local control hub (LCH). Moreover, the Grid interface is supplied with a bidirectional meter, and energy information regarding PV array is also monitored. The LCH receives simple instructions from the "cloud" (the computational server), which runs the control algorithm and the necessary prediction services including daily PV generation forecast (the estimate is calculated from the weather prediction available on OpenWeather

(2019) via solar irradiance prediction model e.g. Seo and Krarti (2011)), home demand forecast (DHW Cylinder, Space Heating and Appliances demand) for each individual dwelling and grid EI forecast, where not provided by the power supplier.

RED WoLF HSS consolidate an energy saving approach in every step and control algorithm focus on the power intake optimisation, with the dwelling power flow included. The battery is allowed to take energy both from the PV array and the Grid, however the control algorithm restricts its discharge to appliances. The choice of preventing batteries from feeding thermal reservoirs avoids round-trip inefficiency. Actually, RED WOLF is designed to predict both the thermal storage and the electrochemical storage that will be required in the next 24/48 hours. Space heating reservoirs, DHW reservoirs and batteries are charged, independently from each other, by both the Grid and the home PV array.

The system design and configuration allow to decrease the average cost of storage significantly per kWh: mid-tier SHs (e.g. Elnur Ecombi HHR) with 24 kWh capacity could cost $\sim$ 500 GBP, weather advanced SHs (e.g. Dimplex Quantum QM150) with 23.1 kWh capacity cost $\sim$ 730 GBP, however a modern Li-ion battery with equal capacity is more than ten times more expensive than this. The estimated price of the mid-tier components and installation of the average system with 2 kWh battery, 4 kW PV array, 5 storage heaters and a water cylinder is $\sim$ 7050 GBP. That is comparable with installation price of gas or oil central heating system, $\sim$ 4000–6000 GBP. Both system are significantly less expensive to ground source heat pump. Telaretti et al. 2016 results suggest that batteries as a sole mechanism for energy storage to shift peak power demand would lead to higher financial expenditures, with exception of TOUT with high level of intra day price difference employed in a dwelling. Furthermore, installation of a heat pump could potentially cost between $\sim$ 13000 – 30000 GBP, which is one order of magnitude higher than installation cost of SHs which could be as low as 0 GBP for simple plug in socket models.

2.2. The Algorithm

Following Shukhobodskiy and Colantuono (2020) we use the progressive threshold approach described therein to operate the HSS. However, with a few modifications. In the algorithm description we use the same notations for variables and parameters as in Shukhobodskiy and Colantuono (2020) with full list presented in nomenclature. This list consists both of predefined parameters, which are directly related to household equipment properties: B_{IMax}, B_{Max}, C_{IMax}, H_{IMax} and $\tilde{H}_{IMax}$. The parameters which are predicted for the next 24/48 hours are P_{P2A}, P_{PV} and Q. T_{TOUT} is assumed to be given in advance for the next 24 hours. Certain variables might be set up in advance by the dweller or automatically predicted for the next 24/48 hours period: C_{Setup} and $\tilde{H}_{Setup}$. The remaining variables are either metered or determined by the algorithm. In contrast to Shukhobodskiy and Colantuono (2020) in this work we consider two possible cases where the the power input to all storage reservoirs could vary continuously from 0 to the nominal power (*Case 1*) and the system were battery still have such a property but SHs and DHW cylinder could only accept nominal power (*Case 2*). Both of these systems could exist in the real world however SHs and DHW cylinders with power intake modulation require additional installation cost.

We start by dividing the algorithm in two stages. *Stage 1* is required to calculate δ, δ_B, δ_{TOUT} and δ_{TOUTB} with the values being updated on hourly basis. The next one *Stage 2* is power flow decision making step updated for each minute.

- *Stage 1*

We define battery demand, SHs and DHW cylinder demand for time period in hours before set up parameters are updated at each $\mathcal{T}$ as

$$\begin{aligned} \tilde{H}_D &= \tilde{H}_{IMax} H(\tilde{H}_{Setup} - \tilde{H}_{level}(\hat{t})), \\ B_D &= B_{IMax} H(B_{Max} - B_{level}(\hat{t})) \quad \text{and} \\ C_D &= C_{IMax} H(C_{Setup} - C_{level}(\hat{t})) \end{aligned} \tag{1}$$

respectively, where $H(x)$ is the Heaviside step function and 0 in the domain of functions corresponds to the start of the day. Then in case $\tilde{H}_{level} \neq \tilde{H}_{Setup}$ within the selected $\mathcal{T}$ hours period we define the integral balance $\mathcal{I}$ as

$$\begin{aligned} \mathcal{I} = \int_{\hat{t}}^{\mathcal{T}} & (P_{P2A}(t) - P_{PV}(t))/60 dt \\ & + C_{Setup} - C_{level}(\hat{t}) + \tilde{H}_{Setup} - \tilde{H}_{level}(\hat{t}), \end{aligned} \tag{2}$$

where t is the time in minutes, $\hat{t}$ is the present time in minutes. Otherwise, in case $\tilde{H}_{level} = \tilde{H}_{Setup}$, we fulfil heat demand and, to avoid overcharging of system, the energy balance simplifies to

$$\begin{aligned} \mathcal{I} = \int_{\hat{t}}^{\mathcal{T}} & (P_{P2A}(t) - P_{PV}(t))/60 dt \\ & + C_{Setup} - C_{level}(\hat{t}). \end{aligned} \tag{3}$$

Equations (2) and (3) represent the difference between energy requirements and energy generation. In case when $\mathcal{I}$ is negative, there is a surplus of energy generated by the PV array in comparison dwelling demand. Thus the grid energy might not be needed. However, in case $\mathcal{I}$ is positive, the energy generated by the PV array does not meet demand; the grid must be use to satisfy dwelling requirements. Such a process enables the estimation of the time of energy intake from the Grid by means of demand and generation forecast, with more energy taken from the Grid for a low PV energy generation forecast and with less energy taken from the grid for a high PV energy generation forecast. That leads to the introduction of the rate of

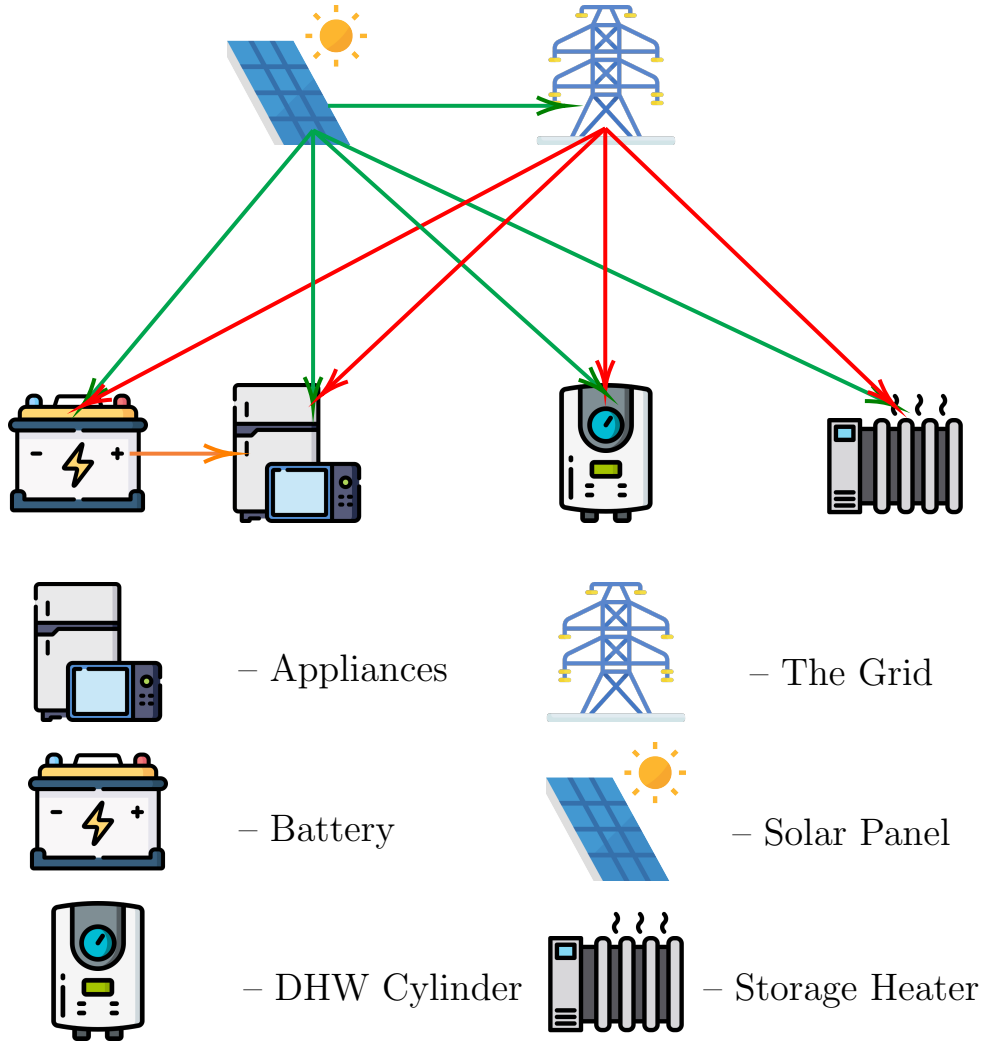

Figure 1: The RED WoLF simplistic symbolic system design and power flow.Red lines correspond to power flow from the Grid, Green lines correspond to power flow from solar panels and yellow line correspond for power flow from a battery. All icons representation are obtained from Flaticon (2020)

power intake:

$$\omega = \frac{\int_{\hat{t}}^{\mathcal{T}} P_{P2A}(t)dt}{\mathcal{T} - \hat{t}} + \tilde{H}_{IMax} + C_{IMax} + B_{IMax}. \quad (4)$$

This allows to define the minimum amount of time of power intake from the Grid $\mathcal{T}_{int}$ for which we allow the external power to be taken as

$$\mathcal{T}_{int} = \left[\max\left(\frac{60\mathcal{I}}{\omega}, \frac{C_{setup} - C_{level}(\hat{t})}{C_{IMax}} \right) \right], \quad (5)$$

where $[x]$ is the nearest integer function of x and $\max(x, y)$ is the maximum function which locates the maximum value between $x \wedge y$. The second term in the right hand side of equation (5) is needed to ensure that charging time is enough to satisfy demand of the water cylinder, in case power generation and consumption forecast is different to actual usage. Then we sort the predicted CO_2 level array Q and TOUT price array T_{TOUT} in order to create arrays in monotonically increasing order Q_{sort} and $T_{TOUTsort}$. As a result we compute EI and price thresholds in order to minimise the power intake from the Grid while satisfying the energy requirements of HSS and appliances. Thresholds are defied as:

$$\delta = Q_{sort}(\mathcal{T}_{int}) \text{ for } \mathcal{I} > 0 \text{ or } \delta = 0 \text{ for } \mathcal{I} \leq 0 \quad (6)$$

and

$$\delta_{TOUT} = T_{TOUTsort}(\mathcal{T}_{int}) \text{ for } \mathcal{I} > 0 \text{ or } \delta_B = 0 \text{ for } \mathcal{I} \leq 0. \quad (7)$$

Furthermore, we introduce the second auxiliary battery threshold which allows the battery to discharge in the most suitable time. We start by calculating the minimum amount of time, for which the battery would be able to

cover appliances consumption demand as

$$\mathcal{T}_B = \mathcal{T} - \hat{t} - \frac{60B_{level}(\hat{t})(\mathcal{T}-\hat{t})}{\int_{\hat{t}}^{\mathcal{T}}(P_{P2A}-P_{PV})dt} \quad \text{when } \exists t \in \mathcal{T} |\ t \leq \hat{t} \quad \tilde{H}_{level}(t) = \tilde{H}_{Setup} \tag{8}$$

and

$$\mathcal{T}_B = \mathcal{T} - \hat{t} - \frac{60B_{level}(\hat{t})(\mathcal{T}-\hat{t})}{\int_{\hat{t}}^{\mathcal{T}}(P_{P2A}-P_{PV})dt - 60\tilde{H}_{Setup}/\mathcal{T}} \quad \text{when } \forall t \in \mathcal{T} |\ t \leq \hat{t} \quad \tilde{H}_{level}(t) \neq \tilde{H}_{Setup}. \tag{9}$$

Equations (8) and (9) allow to disregard heat consumption from battery threshold as soon as daily target for SHs is satisfied and include it once SHs still need to be charged. Now, we are able to define auxiliary battery thresholds both for EI signal and for TOUT price signal as:

$$\delta_B = Q_{sortB}(\mathcal{T}_B) \text{ for } \mathcal{T}_B > 0 \text{ or } \delta_B = 0 \text{ for } \mathcal{T}_B \leq 0 \tag{10}$$

and

$$\delta_{TOUTB} = T_{TOUTsort}(\mathcal{T}_B) \text{ for } \mathcal{T}_B > 0 \text{ or } \delta_{TOUTB} = 0 \text{ for } \mathcal{T}_B \leq 0. \tag{11}$$

The definitions of battery thresholds equations (10) and (11) finalise *Stage 1.*

- *Stage 2*

We are now discussing the 1 minute step procedure in more details. The decision whether to use Grid or not would be defined at any time t by $\delta > Q(t)$ or $\delta \leq Q(t)$ for EI signal or by $\delta_{TOUT} > T_{TOUT}(t)$ or $\delta_{TOUT} \leq T_{TOUT}(t)$ for TOUT price signal. In the following sections this idea is expanded into the two cases - the case with allowed SHs and DHW power modulation and without.

The two-cases framework introduced earlier is hereby analysed, with the heat reservoirs enabled to load either the nominal power only, or any value between zero and such a nominal power

– *Case 1*

In this case power modulation for SHs and DHW Cylinders is allowed. The first case is when $Q(t) \geq \delta$ for the algorithm following EI signal, $T_{TOUT}(t) \geq \delta_{TOUT}$ and also $T_{P2A}(t) \geq T_{PV}(t)$. As a result, PV power does not cover demand and power is drawn from the battery to be used in appliances in case $Q(t) \geq \delta_B$ for the algorithm following EI signal and $T_{TOUT}(t) \geq \delta_{TOUTB}$ for TOUT price signal. Both when battery is insufficient and when battery thresholds is less aligned with the signal trajectory, then the Grid has to satisfy demand for appliance and nothing else will happen unless current SHs level is unable to satisfy heating requirements. The system algorithm is the same for both TOUT price signal and CO_2 signal thus we describe the performance of the system for CO_2 signal only. However, in case we want to operate the system for TOUT price signal we substitute $Q(t)$ with $T_{TOUT}(t)$, δ with δ_{TOUT} and δ_B with δ_{TOUTB}. Then we describe the system performance as:

$$\begin{aligned} T_{PFG} &= (T_{P2A} - T_{PV}) \\ &\quad \times H(T_{P2A}/60 - T_{PV}/60 - B_{level}) \text{ and} \\ T_{PFB} &= (T_{P2A} - T_{PV}) \\ &\quad \times H(T_{P2A}/60 - T_{PV}/60), \\ &\text{when } Q(t) \geq \delta_B \end{aligned} \tag{12}$$

and

$$\begin{aligned} T_{PFG} &= (T_{P2A} - T_{PV}) \\ &\quad \times H(T_{P2A}/60 - T_{PV}/60) \text{ and} \\ T_{PFB} &= (T_{P2A} - T_{PV}) \\ &\quad \times H(T_{P2A}/60 - T_{PV}/60), \\ &\text{when } Q(t) < \delta_B. \end{aligned} \tag{13}$$

Furthermore, in case SHs gets empty due to predictions being different to the measured results we force charge it until next thresholds are calculated in *Stage 1.*

Now, whenever $Q \geq \delta$ and $T_{P2A} \leq T_{PV}$ there is surplus PV generation to satisfy the electrical appliance demand. That yields extra power $E = T_{PV} - T_{P2A}$. Then we have the same four options to deal with the results as in Shukhobodskiy and Colantuono (2020). When $E < C_d$ we put all of the extra power to the DHW cylinder to obtain

$$T_{P2C} = EH(\tilde{H}_{Setup} - C_{level}). \tag{14}$$

Furthermore, in case $E \geq C_D$ and $E < C_D + \tilde{H}_D$ then

$$\begin{aligned} T_{P2C} &= C_D, \\ T_{P2H} &= (E - C_D)H(\tilde{H}_{Setup} - \tilde{H}_{level}). \end{aligned} \tag{15}$$

In this case we have enough power to cover the demand both from appliances and DHW cylinder. However, we do not get enough power to fully satisfy the requirements of SHs. Thus we first direct energy to appliances, then to DHW cylinder and only after it to SHs. Whenever, $E \geq C_D + \tilde{H}_D$ and $E < C_D + \tilde{H}_D + B_D$ the system performance is represented as

$$\begin{aligned} T_{P2C} &= C_D, \\ T_{P2H} &= \tilde{H}_D, \\ T_{P2B} &= \min((E - C_D - \tilde{H}_D), B_{IMax}) \\ &\quad \times H(B_{Max} - B_{level}), \end{aligned} \tag{16}$$

where $\min(x, y)$ is the function that determines minima points $\forall\ x \wedge y$. Now, we have enough power to satisfy all the HSS requirements with exception to battery and thus we first satisfy demand of electrical appliances, then of DHW cylinder, afterwards of SHs and only at latest stage of the battery. Finally, in case $E > C_D + \tilde{H}_D + B_D$, PV

power generation has a surplus to all the demand within the household. Therefore, we are exporting the excess to the Grid, whenever it is allowed. Thus, we obtain

$$\begin{aligned} T_{P2C} &= C_D, \\ T_{P2H} &= \tilde{H}_D, \\ T_{P2B} &= B_D, \\ T_{P2G} &= E - (T_{P2C} + T_{P2H} + T_{P2B}). \end{aligned} \tag{17}$$

Now we move to the case when $Q < \delta$, so that the EI level of the Grid is less than the threshold. In order to continue the description we define the maximum power that can be directed into the dwelling (combination of the Grid and PV generated power) as:

$$M_{HPV} = H_{IMax} + T_{PV}. \tag{18}$$

The EI level of the Grid is less then the threshold. As a result we are free to use cleaner energy from the Grid to satisfy the dwelling demand. However, once the energy level of SHs has reached the target for the day, we restrict them to be charged from the Grid. Hence, whenever $\forall t \in \mathcal{T} |\ t \leq \hat{t} \quad \tilde{H}_{level}(t) \neq \tilde{H}_{Setup}$, yields

$$\begin{aligned} T_{P2C} &= \min(C_D, (M_{HPV} - T_{P2A}) \\ &\quad \times (C_{Setup} - C_{level})), \\ T_{P2H} &= \min(\tilde{H}_D, (M_{HPV} - T_{P2A} - T_{P2C}) \\ &\quad \times H(\tilde{H}_{Setup} - \tilde{H}_{level})), \\ T_{P2B} &= \min(B_D, (M_{HPV} - T_{P2A} - T_{P2C} - T_{P2H}) \\ &\quad \times H(B_{Max} - B_{level})). \end{aligned} \tag{19}$$

Additionally, in case $\exists t \in \mathcal{T} |\ t \leq \hat{t} \quad \tilde{H}_{level}(t) = \tilde{H}_{Setup}$, we have

$$\begin{aligned} T_{P2C} &= \min(C_D, (M_{HPV} - T_{P2A}) \\ &\quad \times (C_{Setup} - C_{level})), \\ T_{P2H} &= \min(\tilde{H}_D, (T_{PV} - T_{P2A} - T_{P2C}) \\ &\quad \times H(\tilde{H}_{Setup} - \tilde{H}_{level})) \text{ for } T_{PV} \geq T_{P2A} + T_{P2C}, \\ T_{P2H} &= 0 \text{ for } T_{PV} < T_{P2A} + T_{P2C}, \\ T_{P2B} &= \min(B_D, (M_{HPV} - T_{P2A} - T_{P2C} - T_{P2H}) \\ &\quad \times H(B_{Max} - B_{level})). \end{aligned} \tag{20}$$

There is also a chance that the system would have excessive PV array generation if $T_{PV} > T_{P2B} + T_{P2H} + T_{P2C}$, then we transit excess of such power into the Grid.

– *Case 2*

In this pathway we consider the house with SHs and DHW cylinders to take power only nominal value or zero. This significantly impacts performance of the first step of the *Stage 2* procedure. However, the main difference to *Case 1* occurs whenever there is not enough power generated by the PV array to satisfy the nominal needs of SHs or DHW cylinder, in which case the energy is transferred to the storage with less nominal requirements. For example in case SHs have insufficient power generated by the PV this energy first tries to satisfy needs of DHW cylinder. However, if power is not sufficient to charge the later, the excess is then directed to the battery or back to the Grid in case battery is at full capacity. This would add additional comparison step to equations (14) – (15). However the rest part of the system would stay the same. As a result, for *Case 2* we change equation (14) to

$$\begin{aligned} T_{P2B} &= EH(B_{Max} - B_{level}), \\ T_{P2G} &= E - T_{P2B}. \end{aligned} \tag{21}$$

Furthermore, we rewrite equation (15)

$$\begin{aligned} T_{P2C} &= C_D, \\ T_{P2B} &= (E - C_D), \\ T_{P2G} &= E - (T_{P2B} + T_{P2C}). \end{aligned} \tag{22}$$

We finally have completed the description of the progressive threshold approach used with the RED WoLF algorithm which is running for 24/48 hour period based on predictions for PV power generation, predictions of the household consumption and of the EI level or TOUT price plan. In sumary, the algorithm is divided in two separate stages *Stage 1* and *Stage 2*. In the latest two cases were presented the one which allows fractional power to enter to SHs and a DHW cylinder *Case 1* and another one, that does not allow power modulations to SHs and a DHW cylinder *Case 2*. The presented algorithm is an improvement of the originally proposed progressive threshold approach described in Shukhobodskiy and Colantuono (2020). The main difference to the original one is the introduction of an auxiliary battery threshold, which improves the performance of the battery within the system. Once again the system decisions are based on whether the main threshold is above the signal level or not. In case when the main threshold is above the target signal level, the Grid is allowed to charge all the storage reservoirs if the PV array alone cannot satisfy the dwelling demand and storage requirements. On the other hand, whenever the main threshold is below a target signal level the grid is only restricted to satisfy the appliance demand, as long as there is shortage of PV generated power, the battery level is insufficient to satisfy demand or the battery is restricted to supply electricity. Furthermore, the Grid could be used to charge SHs as soon as they become empty. Moreover, the added auxiliary battery threshold allows to decide whether to use battery to satisfy the demand in appliances or not. The charging hierarchy stayed the same. In case there is an excess of PV generation, the system would first charge the DHW cylinder, then SHs and only afterwards the battery. If PV is unable to power one of the elements due to restricting non variable power intake this energy would be directed to the battery. Finally, all the excess from PV generation would be exported to the Grid. Figure 2, summarises the logic behind the progressive threshold ap-

proach algorithm, with all of the above details could be tacked in graphical representation.

3. Comparison of RED WoLF system performance for CO_2 and Price targets

In this section we are testing the system behaviour on existing data. We conduct a numerical experiment and simulate system performance during 11 months period from February to December. The PV power generation and consumption profile are taken from Oxford PV array (2016) and Lichman (2013), respectively. These datasets were previously used in studies performed by Colantuono et al. (2018) and Shukhobodskiy and Colantuono (2020). The PV power generation data was recorded in the dwelling in Oxford, UK (Oxford PV array (2016)). The two Grid CO_2 signals considered in the experiment correspond to the UK national intensity levles in 2019 and to London intensity levels in 2019 Carbon Intensity (2020). The data for TOUT tariff represents the price structure provided by the Octopus energy agile tariff Ocotpus Energy (2020) for London in 2019. We also note that the consumption data Lichman (2013), that is coming from the dwelling in France, have been already detrended and seasonal dependence was removed. Moreover, the consumption data is normalised to satisfy 5 MWh annual Grid energy usage, which is very close to the average value in the UK (Enerdata (2019), for comparison the lowest European yearly consumption is in Romania $\approx$ 1.5 MWh, and the highest is in Sweden with $\approx$ 10 MWh annual consumption).

In order to add variability to the system we treat the measured data for PV generation and appliance consumption as predicted time series. Furthermore, we assume that the actual values for consumption and power production could be constructed as $T_{P2A} = |P_{P2A} + \gamma|$ and $T_{PV} = |P_{PV} + \kappa|$, where γ and κ are normally distributed random numbers generated by Python procedure numpy.random.uniform$(-1, 1, (\mathcal{T}, 1))$. That procedure allows to alter the prediction for the true values in every single case. Though that procedure might not be the most accurate in a physical sense it allows us to prove stability of the system. We should note that in case T_{PV} is calculated to be greater than the maximum possible power input from the PV array, we clip it down to its nominal maximum. Furthermore, we vary the battery capacity from 0 kWh to 10 kWh as well as we scale the PV array system from 0 P_{PV} to 4 P_{PV}, which correspond to 0 kW and 16 kW PV system.

Now, we assume that the heating period starts in October and finishes in March. The heat demand is gradually distributed from 0 kWh per day in October to 80 kWh in January to 0 kWh in March and the rest of the year. Furthermore we assume that the heat is used evenly throughout the day. We also assume that the capacity and the daily usage of the DHW cylinder is 10.5 kWh. Also, we assume that the DHW cylinder is used evenly during two disjoint time intervals: 07:00 – 07:50 and 17:30 – 18:20. The Grid power intake of the dwelling is limited to 25 kW (an average UK house has 30/32 A, ring circuits per floor and 52 A circuit for cooker). Such a restriction limits the supply which appliances, SHs, DHW cylinder and battery can take from the Grid.

Below we analyse the new RED WoLF algorithm. We start with performance comparison between the old version Shukhobodskiy and Colantuono (2020) and the one described in section 2 using national CO_2 level in the UK for various PV array and battery sizes. The comparison results are presented in table 1. We can see that the system performance has been significantly improved in the newest version. Furthermore, in case when export of PV power is allowed the system could result in negative CO_2 throughout the study period, reducing the overall EI on the Grid. If export to Grid is allowed, the export can go anywhere: to nearby dwellings but also to other users like factories, traffic lights, hospitals. A version of RED WoLF was also thought for clustering dwellings together but is not the case analysed in this manuscript.

We can see from figure 3 that there is a trend: increase in battery capacity could lead to significant improvements of relative savings. This is because of the significant boost in performance due to implementation of auxiliary battery threshold, that chooses better timing for battery discharge. The auxiliary thresholds provides more flexible control over the battery. Thus better entails the usage of a given capacity. Moreover, even in the absence of PV array and battery, we witness an overall improvement in algorithm performance. That is due to restricting the daily charge of the SHs to its daily target. As a result, SHs do not overcharge during times of high Grid's EI. The overall increase in relative savings due to increase or decrease in PV array's size is non-linear. The systems equipped with a PV array generating much lower power than appliance consumption are showing the best relative gain in performance. Hence, it can be considered that the correct timing for charging the battery, SHs and a DHW cylinder from the Grid has significantly higher effect on low generation systems. On the other hand, this effect is less important when we have insufficient or comparable power generation to system consumption. However it becomes more pronounced for systems with surplus of energy produced by renewable source.

We should note that running 11 months simulation with 1 minute resolution time takes $\approx$ 10 minutes to execute in case only one target is considered and $\approx$ 20 minutes if two targets are calculated simultaneously. This reference is given for a system equipped with Intel(R) Core(TM) i7-8700 CPU with 32 GB RAM, with script written on Python via SPYDER 4.0.1. GUI. We then use primal-dual simplex method (Curet, 1993; Lau et al., 2018) in order to find maximum amount of possible savings in the idealised case. Preprocessing procedure (Nacedal and Wright (2006)) is employed before optimisation to simplify the problem by removing redundancies and simplifying con-

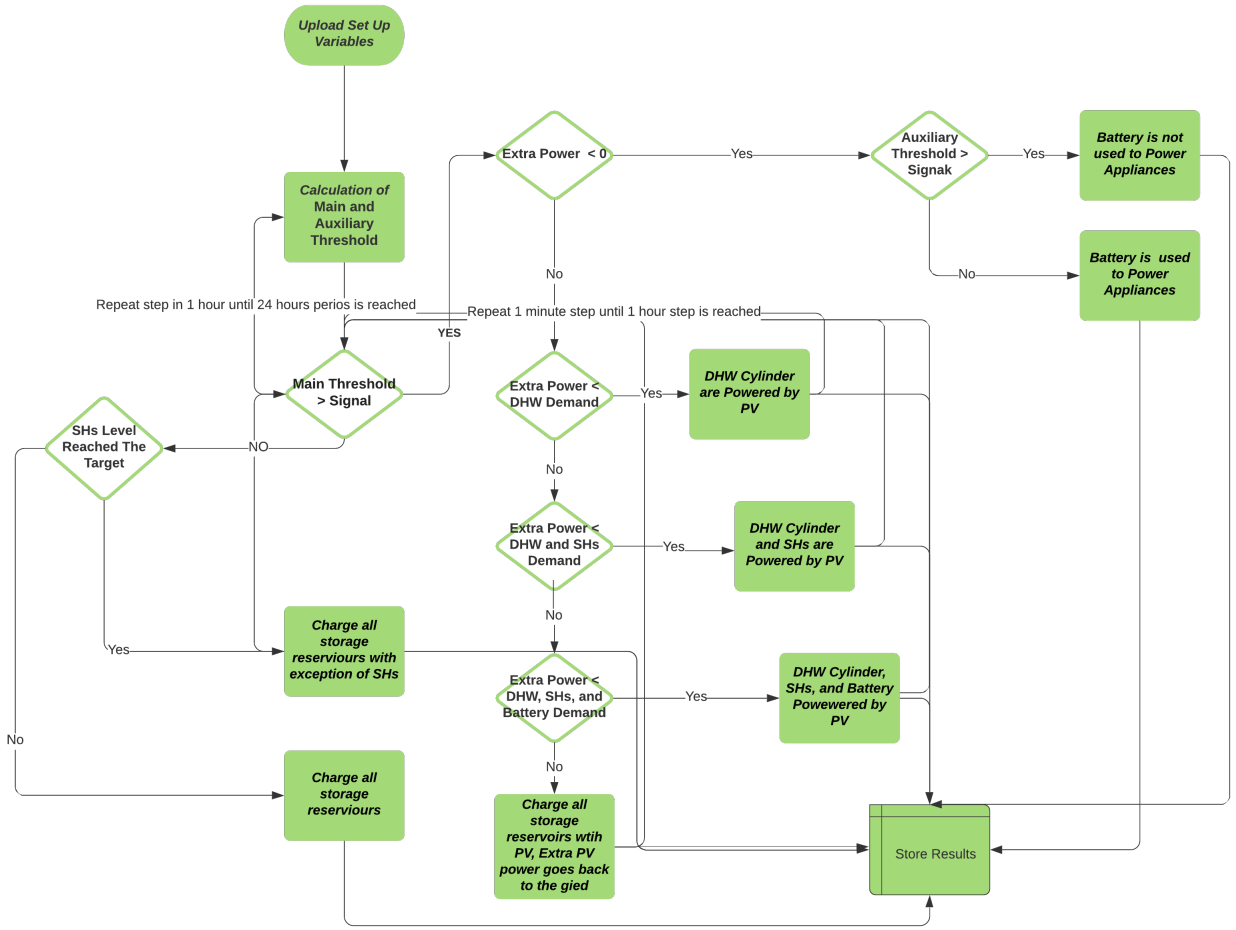

Figure 2: Progressive threshold approach logic scheme employed in the RED WoLF HSS.

strains. For that simulation we also assume that predictions are error free and the system is composed of ideal elements. In addition, due to much higher computational needs, instead of the resolution of 1 min, we use 1 hour steps. Furthermore, all the data for the investigated time period is considered to be known in advance. In this case 11 months simultaneous computation takes ≈ 8 minutes. We could see from figure 4 that the maximum limit on the RED WoLF system is only $\approx 8 - 14$ % higher to the values obtained with progressive threshold approach and it would be mathematically impossible to get higher values. Furthermore, all the trends existing in the RED WoLF algorithm are still present. Nevertheless, such approach could not be realised in the real life situation due to absence of accurate predictions further than 24 hour period and idealistic equipment. We then estimated the time needed to compute 11 months period, in day by day with hourly recalculation. That recalculation emulates the response to possible errors due to differences in prediction and measured data. As a result, we the time of calculation with 1 minute step resolution is ≈ 2489 minutes and the time of calculation with 1 hour resolution is ≈ 60 minutes. Both computation time intervals are much higher than the one of the progressive threshold approach.

In what follows we analyse the impact on the overall environmental and price benefits of the system by following TOUT price target or EI target. Time series describing the system simulation over the fourteen days in February in London for both CO_2 and TOUT price signals for the system with 4 kW PV array and 5 kWh Battery is presented in figure 5. Evidently there are two important aspects of the system performance. First of all, once SHs reach the daily target they stop charging from the Grid. The second observation is that the auxiliary battery threshold leads to discharge of the system when the target signals are relatively high. Both of these facts confirm that the system is working as intended. Furthermore, we can see in figure 5 that there is some resemblance in system performance by following one or another signal. Nevertheless, some differences are present. As a result, we continue the work by investigating this effect on the 11 months period for *Case 1* and *Case 2* algorithms.

	10 kWh Battery	7 kWh Battery	5 kWh Battery	2 kWh Battery	0 kWh Battery
RED WoLF Old 16 kW PV	1645 kg	1656 kg	1670 kg	1708 kg	1788 kg
RED WoLF 16 kW PV	1145 kg	1187 kg	1206 kg	1261 kg	1370 kg
RED WoLF Export 16 kW PV	−507 kg	−489 kg	−485 kg	−464 kg	−370 kg
RED WoLF Old 8 kW PV	1846 kg	1860 kg	1874 kg	1910 kg	1975 kg
RED WoLF 8 kW PV	1381 kg	1420 kg	1436 kg	1489 kg	1602 kg
RED WoLF Export 8 kW PV	773 kg	797 kg	803 kg	838 kg	941 kg
RED WoLF Old 4 kW PV	2077 kg	2094 kg	2120 kg	2143 kg	2191 kg
RED WoLF 4 kW PV	1589 kg	1624 kg	1660 kg	1704 kg	1813 kg
RED WoLF Export 4 kW PV	1414 kg	1440 kg	1464 kg	1497 kg	1603 kg
RED WoLF Old 2 kW PV	2336 kg	2356 kg	2372 kg	2402 kg	2419 kg
RED WoLF 2 kW PV	1765 kg	1808 kg	1847 kg	1899 kg	2003 kg
RED WoLF Export 2 kW PV	1739 kg	1770 kg	1799 kg	1847 kg	1951 kg
RED WoLF Old 0 kW PV	2760 kg	2785 kg	2800 kg	2825 kg	2813 kg
RED WoLF 0 kW PV	2120 kg	2159 kg	2192 kg	2248 kg	2350 kg
RED WoLF Export 0 kW PV	2120 kg	2159 kg	2192 kg	2248 kg	2350 kg
No RED WoLF 0 kW PV	–	–	–	–	3590 kg

Table 1: The performance comparison between the old and the new versions of the RED WoLF algorithm for the 11 months period from February till December. The values inside table correspond to the Grid CO_2 output of the dwelling. Columns correspond to variation in battery capacity between 10 kWh – 0 kWh. Rows correspond to variation in PV array size between 16 kW – 0 kW. RED WoLF Old, RED WoLF, RED WoLF Export correspond to old version of the RED WoLF algorithm and No RED WoLF, new version of the RED WoLF algorithm, new version of the RED WoLF algorithm with export of excess PV energy allowed and the house with same consumption profile without any storage system respectively.

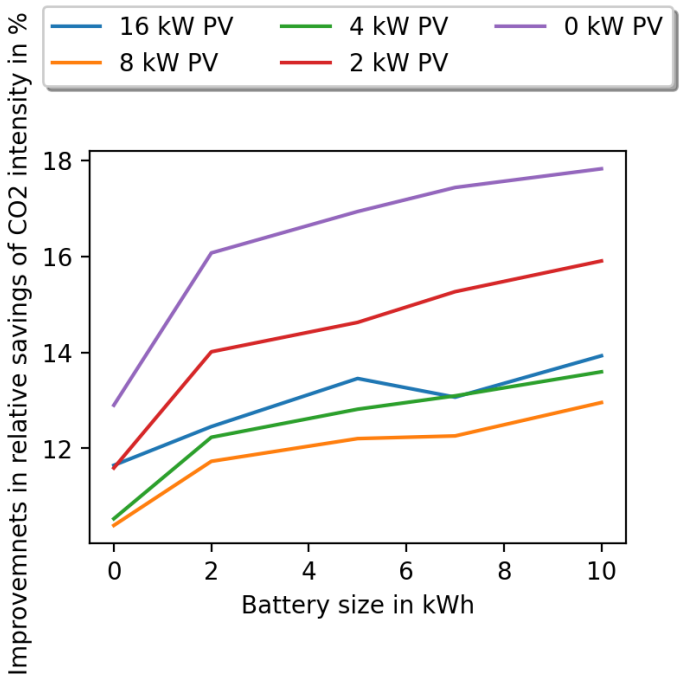

Figure 3: Dependence of improvements in relative savings of CO_2 by implementing the new version of the algorithm on the battery size. The purple, red, green, orange and blue lines corresponds to 0 kW, 2 kW, 4 kW, 8 kW and 16 kW PV arrays respectively.

We start investigation by performing numerical simulation for *Case 1* settings. The results of 11 months experiment are presented in table 2. In addition the conclusion we can make from the table is that following any signal be it EI or TOUT price result in savings in both applied algorithm targets. Furthermore, even in absence of battery storage and PV array the system provides $\approx 45\%$ reduction of the followed target. The dependence of relative savings on the battery and PV array sizes is presented on top of figure 6. The results could be summarised as follows. As expected an increase in battery capacity leads to increase in relative saving. A similar effect could be seen in case PV arrays are enlarged. Depending on the HSS properties the savings could vary from just under $\approx 45\%$ for systems with absence of a PV array and battery to just over $\approx 70\%$ for systems with a large PV array and high capacity battery. In most cases the increase in PV array size improves the system much more significantly than increasing the size of a battery. However, in some cases (e.g., for the RED WoLF system following price signal) the system with higher battery capacity was able to outperform the system.

The bottom of Fig. 7 suggests that following the TOUT price signals strongly impacts also CO_2 emissions, from $\approx 6\%$ to $\approx 14\%$, depending on the system size. On the other hand, the resulting price is significantly less affected when the algorithm follows the grid EI signal. The difference between following EI and TOUT price signal is $\approx 1.5\%$ to $\approx 4.5\%$. Moreover, the overall trend suggests that the increase in battery capacity makes this effect more prominent. However, increase in the PV system size may lead to reduction of that trend for overall savings for red EI. Moreover, such effect is not observable for the price. It also seems that in case a dweller does not have preference for which target to follow, the CO_2 signal would be a preferable option, since there would be much less discrepancy between the final bill and emissions. Thus, CO_2 emissions of the Grid have stronger influence of the TOUT

	10 kWh Battery	7 kWh Battery	5 kWh Battery	2 kWh Battery	0 kWh Battery
RED WoLF CO_2 Follow Price 16 kW PV	672.5 GBP	684.5 GBP	695.3 GBP	717.1 GBP	754.0 GBP
RED WoLF Price Follow Price 16 kW PV	613.0 GBP	631.2 GBP	647.4 GBP	668.7 GBP	704.4 GBP
RED WoLF CO_2 Follow CO_2 16 kW PV	1126 kg	1148 kg	1161 kg	1200 kg	1279 kg
RED WoLF Price Follow CO_2 16 kW PV	1380 kg	1431 kg	1453 kg	1493 kg	1488 kg
RED WoLF CO_2 Follow Price 8 kW PV	793.1 GBP	807.4 GBP	817.9 GBP	832.6 GBP	876.1 GBP
RED WoLF Price Follow Price 8 kW PV	726.1 GBP	745.6 GBP	760.4 GBP	784.9 GBP	814.4 GBP
RED WoLF CO_2 Follow CO_2 8 kW PV	1302 kg	1325 kg	1345 kg	1369 kg	1455 kg
RED WoLF Price Follow CO_2 8 kW PV	1644 kg	1691 kg	1705 kg	1723 kg	1734 kg
RED WoLF CO_2 Follow Price 4 kW PV	893.3 GBP	909.0 GBP	920.4 GBP	938.6 GBP	981.9 GBP
RED WoLF Price Follow Price 4 kW PV	824.5 GBP	842.2 GBP	855.6 GBP	890.9 GBP	921.3 GBP
RED WoLF CO_2 Follow CO_2 4 kW PV	1476 kg	1498 kg	1518 kg	1554 kg	1639 kg
RED WoLF Price Follow CO_2 4 kW PV	1898 kg	1921 kg	1941 kg	1964 kg	1986 kg
RED WoLF CO_2 Follow Price 2 kW PV	979.1 GBP	1002.3 GBP	1010.0 GBP	1030.6 GBP	1075.4 GBP
RED WoLF Price Follow Price 2 kW PV	910.4 GBP	927.6 GBP	947.6 GBP	985.4 GBP	1011.8 GBP
RED WoLF CO_2 Follow CO_2 2 kW PV	1618 kg	1652 kg	1668 kg	1721 kg	1819 kg
RED WoLF Price Follow CO_2 2 kW PV	2078 kg	2103 kg	2135 kg	2186 kg	2192 kg
RED WoLF CO_2 Follow Price 0 kW PV	1146.9 GBP	1161.0 GBP	1184.5 GBP	1209.9 GBP	1245.7 GBP
RED WoLF Price Follow Price 0 kW PV	1045.2 GBP	1066.9 GBP	1090.4 GBP	1155.1 GBP	1202.9 GBP
RED WoLF CO_2 Follow CO_2 0 kW PV	1917 kg	1940 kg	1978 kg	2041 kg	2130 kg
RED WoLF Price Follow CO_2 0 kW PV	2452 kg	2467 kg	2492 kg	2557 kg	2560 kg
No RED WoLF Price 0 kW PV	–	–	–	–	2157.8 GBP
No RED WoLF CO_2 0 kW PV	–	–	–	–	3744 kg

Table 2: The results of 11 months numerical simulation for *Case 1* of the RED WoLF system. The rows correspond to variation of a PV array between 16 kW – 0 kW and target signal. Columns correspond to variation of a battery capacity between 10 kWh – 0 kWh. RED WoLF CO_2 Follow Price corresponds to the final bill price, while system follows CO_2 signal. RED WoLF Price Follow Price corresponds to the final bill price, while system follows TOUT price target. RED WoLF CO_2 Follow CO_2 corresponds to the Grid CO_2 emissions, in case system follows EI signal. RED WoLF price Follow CO_2 to the Grid CO_2 emissions, with system following TOUT price signal. No RED WoLF Price corresponds to the final bill price without RED WoLF HSS being present, however the dwelling has the same consumption profile. No RED WoLF CO_2 corresponds to the Grid CO_2 emission without, HSS being implemented.

price. Meaning, that EI could be a crucial factor for price generation. On the contrary TOUT price distribution has much weaker influence on the EI distribution. One of the reason of why such phenomena can occur is that sustainable energy sources, like nuclear, solar and wind have much lower or non-existent EI output. In addition, while excess wind and solar are always both green and cheap, if not wholesale negative (i.e., if one follows CO_2 one might also get financial advantage), some high carbon electricity (e.g. inflexible fossil fuel pants) can be cheap as well at time of low demand. In fact, Economy 7 was cheap also last century (when used to be extremely dirty) due to coal plant's inflexible generation coupled to lack of demand. Therefore, nowadays, you can still take cheap but dirt electricity. Nevertheless, there is price associated with energy production, which impacts price distribution of TOUT tariff.

Table 3 presents the performance of RED WoLF system for *Case 2* scenario, where SHs and a DHW cylinder are not able to take fractional power. The results show increase in the overall 11 months bill and CO_2 emissions in comparison with the system performance for *Case 1*. Figure 8 illustrates such comparison. There is no difference between two cases when there is no PV array. Moreover, the general trend is, the higher the battery size the lower is the difference. On the contrary, the larger PV arrays tend to increase the difference between the resulting output. The explanation to such intriguing occurrence is simple. PV output can fluctuate, whereas the grid output could be monotonic. These lead to accumulation of error, with larger PV systems producing higher amplitudes for the power generation output. As a result, such an instability slightly reduces the performance of the RED WoLF system. Nevertheless, the resulting savings for *Case 2* are promising. It follows from figure 9 that the system savings in case CO_2 signal followed varies between $\approx 42\%$ to $\approx 62\%$. Whether, relative savings for RED WoLF system employing TOUT price signal vary between $\approx 45\%$ to $\approx 65\%$. The system has the same overall properties as the *Case 1* system. The higher the battery capacity and the PV array generation are, the less the price and the Grid CO_2 emissions are. However, there is a difference we could immediately spot is that systems with comparatively lower PV array but with the higher battery capacity can outperform the systems with comparatively lower PV array and lower battery capacity. Thus, we can conclude that battery is more influential for *Case 2* systems. Finally, it follows from figure 10 that the change of target signal has a more prominent effect on EI savings.

	10 kWh Battery	7 kWh Battery	5 kWh Battery	2 kWh Battery	0 kWh Battery
RED WoLF CO_2 Follow Price 16 kW PV	795.9 GBP	811.8 GBP	829.9 GBP	869.0 GBP	900.9 GBP
RED WoLF Price Follow Price 16 kW PV	750.8 GBP	766.1 GBP	784.1 GBP	832.1 GBP	875.9 GBP
RED WoLF CO_2 Follow CO_2 16 kW PV	1370 kg	1397 kg	1430 kg	1517 kg	1565 kg
RED WoLF Price Follow CO_2 16 kW PV	1677 kg	1704 kg	1733 kg	1811 kg	1859 kg
RED WoLF CO_2 Follow Price 8 kW PV	871.3 GBP	885.4 GBP	898.1 GBP	935.1 GBP	958.9 GBP
RED WoLF Price Follow Price 8 kW PV	788.7 GBP	807.6 GBP	823.2 GBP	872.5 GBP	912.6 GBP
RED WoLF CO_2 Follow CO_2 8 kW PV	1452 kg	1470 kg	1495 kg	1571 kg	1617 kg
RED WoLF Price Follow CO_2 8 kW PV	1796 kg	1830 kg	1854 kg	1926 kg	1970 kg
RED WoLF CO_2 Follow Price 4 kW PV	966.4 GBP	980.7 GBP	997.2 GBP	1031.6 GBP	1057.3 GBP
RED WoLF Price Follow Price 4 kW PV	881.3 GBP	899.9 GBP	916.0 GBP	962.9 GBP	1004.1 GBP
RED WoLF CO_2 Follow CO_2 4 kW PV	1617 kg	1645 kg	1675 kg	1746 kg	1789 kg
RED WoLF Price Follow CO_2 4 kW PV	2008 kg	2042 kg	2069 kg	2138 kg	2180 kg
RED WoLF CO_2 Follow Price 2 kW PV	1027.1 GBP	1046.6 GBP	1062.5 GBP	1089.2 GBP	1126.1 GBP
RED WoLF Price Follow Price 2 kW PV	934.2 GBP	957.4 GBP	976.4 GBP	1026.7 GBP	1067.4 GBP
RED WoLF CO_2 Follow CO_2 2 kW PV	1707 kg	1734 kg	1763 kg	1831 kg	1910 kg
RED WoLF Price Follow CO_2 2 kW PV	2146 kg	2182 kg	2206 kg	2276 kg	2319 kg
RED WoLF CO_2 Follow Price 0 kW PV	1146.9 GBP	1161.0 GBP	1184.5 GBP	1209.9 GBP	1245.7 GBP
RED WoLF Price Follow Price 0 kW PV	1045.2 GBP	1066.9 GBP	1090.4 GBP	1155.1 GBP	1202.9 GBP
RED WoLF CO_2 Follow CO_2 0 kW PV	1917 kg	1940 kg	1978 kg	2041 kg	2130 kg
RED WoLF Price Follow CO_2 0 kW PV	2452 kg	2467 kg	2492 kg	2557 kg	2560 kg
No RED WoLF Price 0 kW PV	–	–	–	–	2157.8 GBP
No RED WoLF CO_2 0 kW PV	–	–	–	–	3744 kg

Table 3: The results of 11 months numerical simulation for *Case 2* of the RED WoLF system. The rows correspond to variation of a PV array between 16 kW – 0 kW and target signal. Columns correspond to variation of a battery capacity between 10 kWh – 0 kWh. RED WoLF CO_2 Follow Price corresponds to the final bill price, while system follows CO_2 signal. RED WoLF Price Follow Price corresponds to the final bill price, while system follows TOUT price target. RED WoLF CO_2 Follow CO_2 corresponds to the Grid CO_2 emissions, in case system follows EI signal. RED WoLF price Follow CO_2 to the Grid CO_2 emissions, with system following TOUT price signal. No RED WoLF Price corresponds to the final bill price without RED WoLF HSS being present, however the dwelling has the same consumption profile. No RED WoLF CO_2 corresponds to the Grid CO_2 emission without, HSS being implemented.

4. Conclusion

We expand the idea of the progressive threshold approach implemented in the RED WoLF hybrid storage system in order to not only reduce CO_2 emissions of the electrical grid employed in residential dwellings, but also the bill for time of use tariff. CO_2 reduction can be achieved by adding renewable energy generator in form of a PV system and by storing the energy whenever EI of the grid or price of time of use tariff is low (Shukhobodskiy and Colantuono (2020)). The reserved energy is later exploited whenever EI or price of time of use tariff is high. The operational decision of whether to reserve or employ the stored energy is achieved by following the progressive threshold approach.

The progressive threshold approach has being substantially improved. The performed numerical experiment on the existing data of the UK national EI, a dwelling consumption, and the PV power generation, the newest progressive threshold approach improves the performance of the RED WoLF system by increasing the overall savings from $\approx 11\%$ to $\approx 18\%$, depending on system configuration, thank to new auxiliary threshold. The savings achieved by the proposed method are only $\approx 8\%$ to $\approx 14\%$ lower to the mathematical maximum for the idealistic equipment and perfect predictions case. Furthermore, the computation time is ≈ 248 faster then the one achieved with primal-dual simplex method.

The newest method is later applied in numerical experiment employing London Grid EI signal and price data for London provided by pioneering in the UK Octopus energy time of use tariff. The first test was performed on the RED WoLF system with storage heaters and hot water cylinder allowing the fractional power intake. Another test was performed on systems allowing only nominal power for the thermal storage reservoir. In both cases the results show significant reduction in the bill and in house's CO_2 emissions. In the first case, where fractional power is allowed, the overall savings of CO_2 vary from $\approx 45\%$ to 70%. Similar values are achieved by the system for overall price reduction in case when the time of use tariff is applied as a target. The test performed for systems without fractional power intake allowed by storage heaters and domestic hot water cylinder presents slightly lower reduction. It follows from the performed comparison between the two systems that the drop in savings is from $\approx 8\%$ to 0%. Moreover, the general conclusion is the gradual increase in PV size leads to a gradually smaller gain in total savings. Furthermore, the systems equipped with batteries of larger capacities reduce the difference between the two possible system configurations. This is because more fractional power could be directed to the the battery with higher capacity. Interestingly, simulation results suggest that effect of battery ageing, would be minor, since the difference in savings for both price and environmental tar-

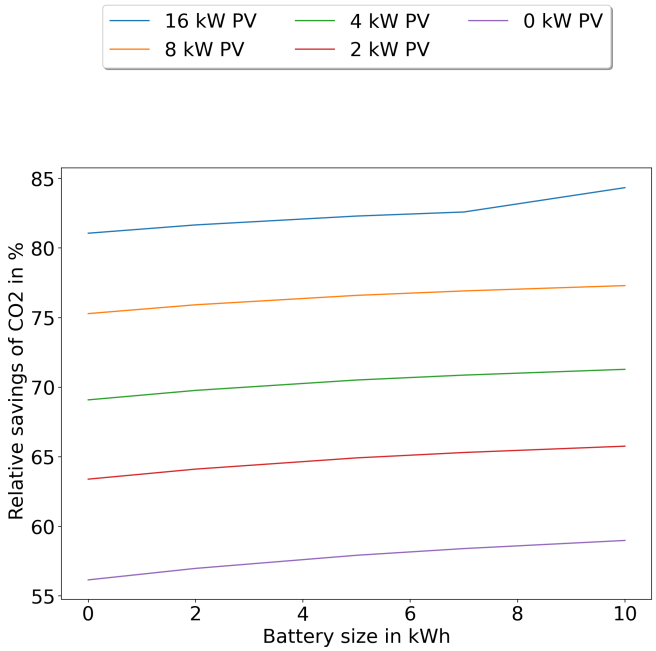

Figure 4: Idealised RED WoLF system performance on national CO_2 signal. The right panel correspond to relative savings in price on battery capacity. Blue, orange, green, red and purple lines are related to systems with 16 kW, 8 kW, 4 kW, 2 kW and 0 kW PV array respectively.

get for systems equipped with 0 kWh battery and 10 kWh battery is typically less than 4 %. This conclusion is different to system with battery as sole storage Muoz-Rodrguez et al. (2021)

Another interesting result was achieved by studying the effect on the outcome by following the "wrong" target. The results were intriguing. The effect of the "wrong" target is more prominent when following the CO_2 signal reaching $\approx 4.5\%$ to $\approx 14\%$ of total decrease in savings. As a result, we can conclude that the EI level of the grid in the UK might have significant impact on price generation. However, the opposite is not true. Potentially due to energy production with lower CO_2 output such as nuclear or renewable, which also comes with associated price. Thus, in case when dweller is interested in achieving both sustainability and reducing the annual bill for the standard system equipped with a 2 kWh battery and a 4 kW PV array the choice would be to follow CO_2 signal as increase in annual bill would be negligible ($\approx$ 7050 GBP for the RED WoLF HSS, $4000 - 6000$ for central heating system).

The results of the numerical experiment are optimistic considering that the values obtained for 11 month period from February to December provide the reference price of 890.9 GBP which is on par or lower to the average annual energy price of 1138 GBP (Ofgem) for a dwelling equipped with gas central heating. Moreover, the CO_2 output of 1518 kg is significantly lower than the lowest 10% earners in the UK with the mean of 3760 kg of CO_2 emissions annually (the reference number for top 10% of the UK earners is 7896 kg of CO_2 in accordance to CSE). Thus, the RED WoLF hybrid storage system, has a great potential to lead to the world to the new era of sustainable energy.

The progressive threshold approach will be tested in pilot sites over couple of years. The resulting dataset would be unique and would allow to estimate both economical and environmental effects of the RED WoLF hybrid storage system.

Nomenclature

Acronyms

CCS	Carbon Capture and Sequestration
DHW	Domestic Hot Water
EU	European Union
EI	Envirnomental Index (CO_2intensity index)
GHG	Green House Gases
HSS	Hybrid Storage System
LCH	Local Control Hub
NWE	North West Europe
PV	Photovoltaic
RED WoLF	Rethink Electricity Distribution Without Load Following
SHs	Storage heaters
The Grid	Electric Grid
The UK	The United Kingdom of Great Britain and Northern Ireland
TOUT	Time of use tariff

Parameters

B_{IMax}	Maximum rate of battery intake in kW
B_{Max}	Maximum battery capacity in kWh
C_{IMax}	Maximum rate of cylinder intake in kW
H_{IMax}	Maximum rate of house intake from Grid in kW
$\tilde{H}_{IMax}$	Maximum rate of heat intake in kW

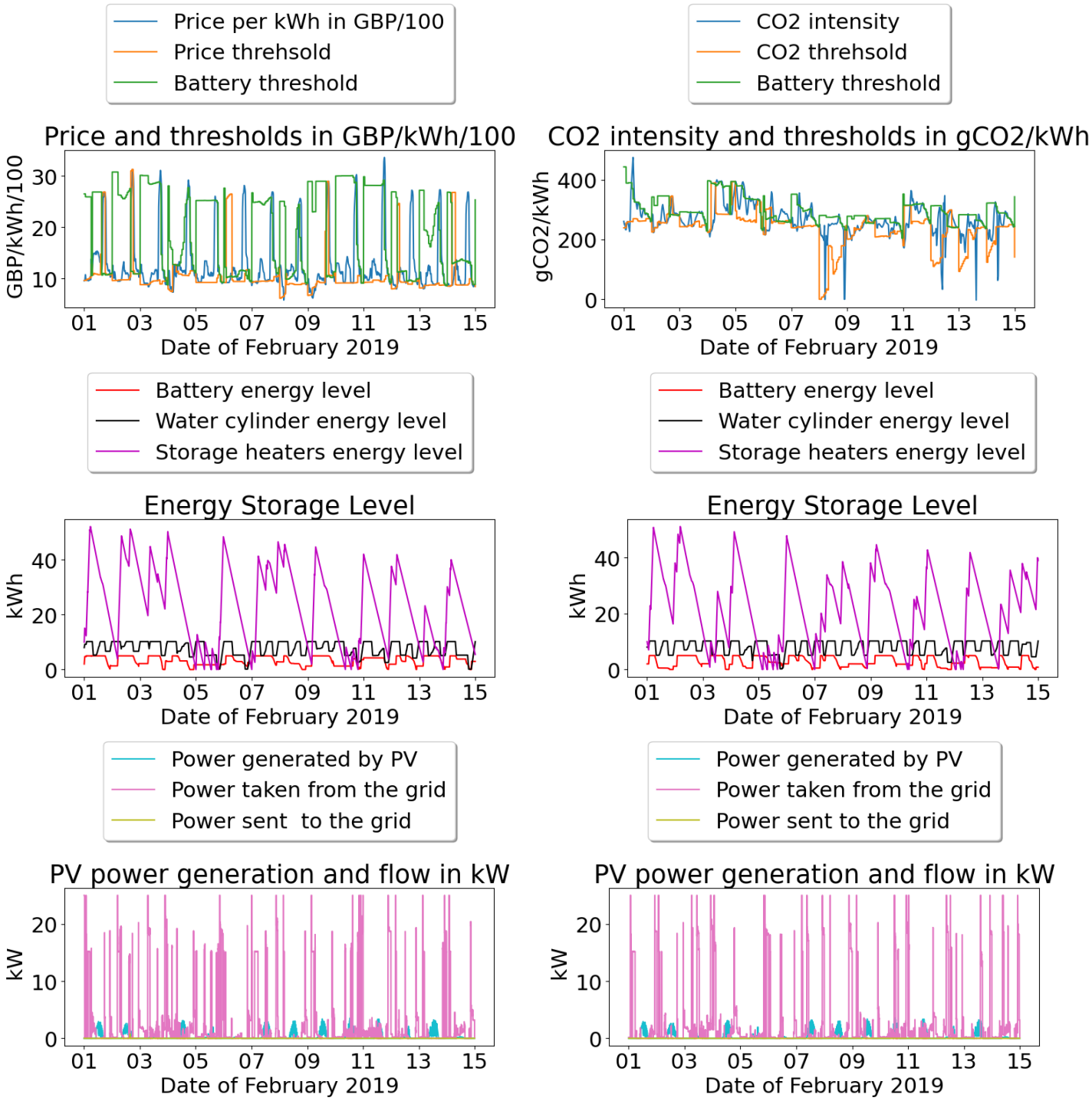

Figure 5: First 14 days of system simulation. Left panels correspond to the system following price signal. Right panels correspond to the system following the Grid EI signal. Top panels display target signals and main and auxiliary thresholds. Middle panels correspond to HSS storage level. Bottom panels correspond to power flow.

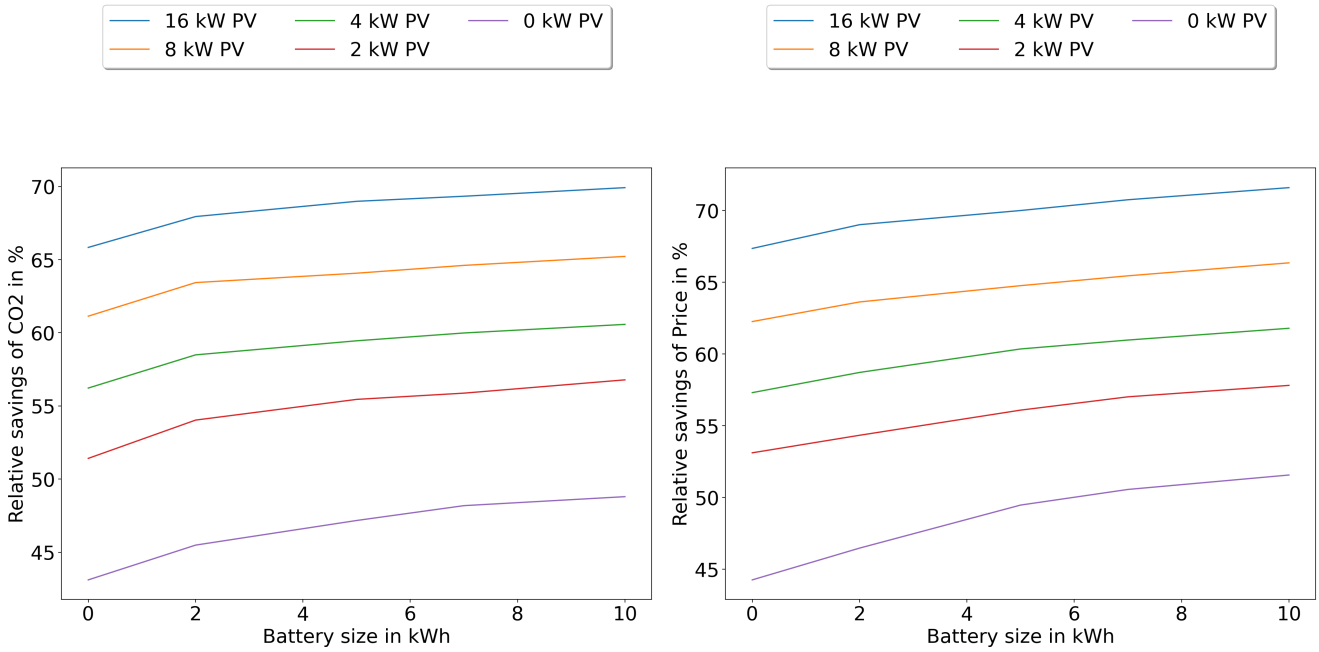

Figure 6: Comparison of RED WoLF system performance for *Case 1* in London. The left panel correspond to dependence of relative savings in CO_2 emissions on battery capacity. The right panel correspond to dependence of improvements of relative savings in price on battery capacity. Blue, orange, green, red and purple lines are related to systems with 16 kW, 8 kW, 4 kW, 2 kW and 0 kW PV array respectively.

Variables

B_D	Battery demand in kW
B_{level}	Battery level in kWh
C_D	DHW cylinder demand in kW
C_{level}	DHW cylinder level in kWh
C_{Setup}	The energy in kWh, that DHW cylinder has to store in 24 hours
$\tilde{H}_D$	Space heating demand in kW
$\tilde{H}_{level}$	Heat level in kWh
$\tilde{H}_{Setup}$	The energy in kWh, that SHs has to store in 24 hours
P_{P2A}	Predicted power to appliance in kW
P_{PV}	Predicted power from PV in kW
T_{PV}	Actual power from PV in kW
T_{P2B}	Actual power to battery in kW
T_{PFB}	Actual power from battery in kW
T_{P2H}	Actual power to heat in kW
T_{P2C}	Actual power to cylinder in kW
T_{PFG}	Actual power from Grid in kW
T_{P2G}	Actual power to Grid in kW
T_{P2A}	Actual power to appliance in kW
T_{TOUT}	Actual price in GBP/kWh of TOUT
Q	CO_2 intensity level prediction in gCO_2/kWh
δ	CO_2 intensity threshold in gCO_2/kWh
δ_B	CO_2 battery threshold in gCO_2/kWh
δ_{TOUT}	TOUT intensity threshold in GBP/kWh
δ_{TOUTB}	TOUT battery threshold in GBP/kWh

Acknowledgemnt

This work has been supported by the European Regional Development Fund, project RED WoLF, project number NWE847 The authors also thank Laura Brown from Leeds Beckett University for language support.

References

Andoni, M., Robu, V., Frh, W.G., Flynn, D., 2017. Game-theoretic modeling of curtailment rules and network investments with distributed generation. Applied Energy 201, 174 – 187.

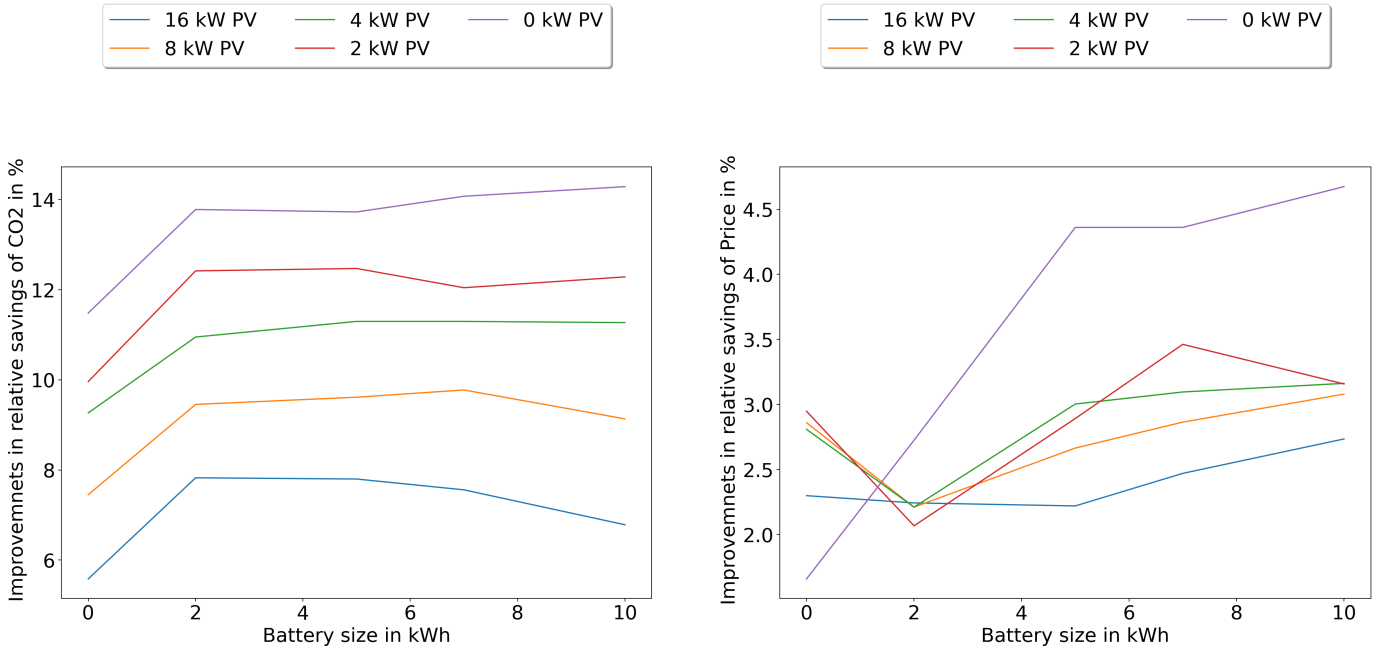

Figure 7: Comparison of RED WoLF system performance for *Case 1* in London. The left panel correspond to dependence of improvements of relative savings in CO_2 emissions on battery capacity, by the algorithm following EI signal instead of TOUT price signal. The right panel correspond to dependence of improvements of relative savings in price on battery capacity, with the algorithm following TOUT price signal instead of environmental signal. Blue, orange, green, red and purple lines are related to systems with 16 kW, 8 kW, 4 kW, 2 kW and 0 kW PV array respectively.

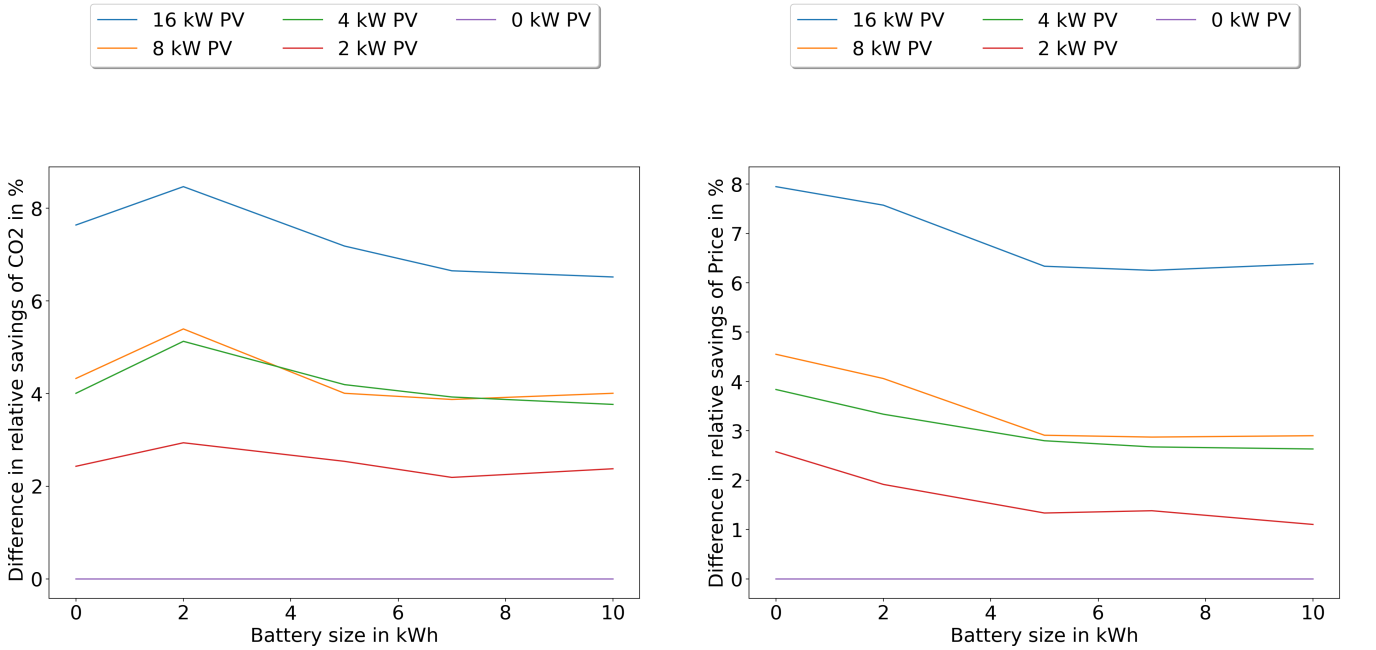

Figure 8: Difference of RED WoLF system performance between *Case 2* and *Case 1* in London. The left panel correspond to dependence of the difference of relative savings in CO_2 emissions on battery capacity. The right panel correspond to dependence of the difference of relative savings in price on battery capacity. Blue, orange, green, red and purple lines are related to systems with 16 kW, 8 kW, 4 kW, 2 kW and 0 kW PV array respectively.

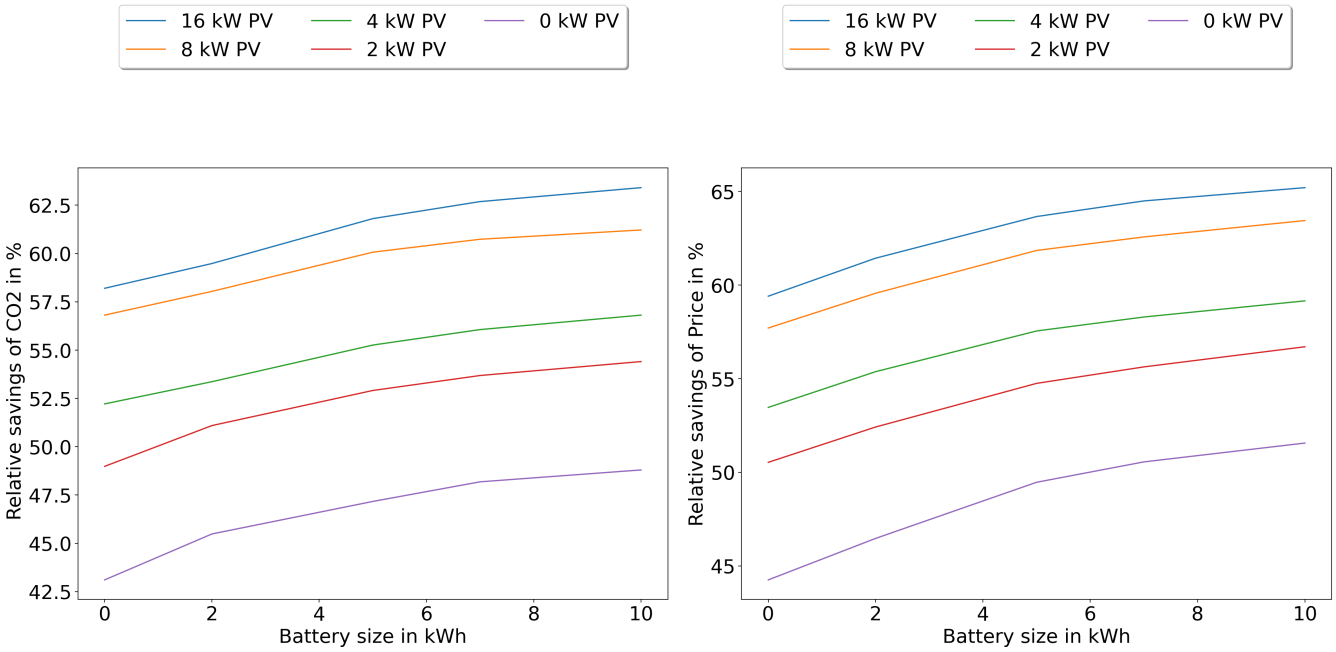

Figure 9: Comparison of RED WoLF system performance for *Case 2* in London. The left panel correspond to dependence of relative savings in CO_2 emissions on battery capacity. The right panel correspond to dependence of improvements of relative savings in price on battery capacity. Blue, orange, green, red and purple lines are related to systems with 16 kW, 8 kW, 4 kW, 2 kW and 0 kW PV array respectively.

Arani, A.K., Gharehpetian, G.B., Abedi, M., 2019. Review on energy storage systems control methods in microgrids. International Journal of Electrical Power & Energy Systems 107, 745 – 757. doi:https://doi.org/10.1016/j.ijepes.2018.12.040.

Baeten, B., Rogiers, F., Helsen, L., 2017. Reduction of heat pump induced peak electricity use and required generation capacity through thermal energy storage and demand response. Applied Energy 195, 184 – 195. URL: http://www.sciencedirect.com/science/article/pii/S0306261917302854, doi:https://doi.org/10.1016/j.apenergy.2017.03.055.

Baniasadi, A., Habibi, D., Al-Saedi, W., Masoum, M.A., Das, C.K., Mousavi, N., 2020. Optimal sizing design and operation of electrical and thermal energy storage systems in smart buildings. Journal of Energy Storage 28, 101186. doi:https://doi.org/10.1016/j.est.2019.101186.

Carbon Intensity, 2020. Carbon intensity api. URL: https://carbonintensity.org.uk/.

Colantuono, G., Kor, A.L., Pattinson, C., Gorse, C., 2018. PV with multiple storage as function of geolocation. Solar Energy 165, 217–232. doi:10.1016/j.solener.2018.03.020.

CSE, . Center for sutainable energy. URL: www.cse.org.uk.

Curet, N.D., 1993. A primal-dual simplex method for linear programs. Operations Research Letters 13, 233–237. URL: https://www.sciencedirect.com/science/article/pii/016763779390045I, doi:https://doi.org/10.1016/0167-6377(93)90045-I.

Ederer, N., 2015. The market value and impact of offshore wind on the electricity spot market: Evidence from germany. Applied Energy 154, 805 – 814.

Enerdata, 2019. Enerdata intelligence + Consulting. https://www.odyssee-mure.eu/publications/efficiency-by-sector/households/electricity-consumption-dwelling.html.

Felten, B., Weber, C., 2018. The value(s) of flexible heat pumps assessment of technical and economic conditions. Applied Energy 228, 1292 – 1319. URL: http://www.sciencedirect.com/science/article/pii/S0306261918309000, doi:https://doi.org/10.1016/j.apenergy.2018.06.031.

Flaticon, 2020. Flaticon.com. URL: https://Flaticon.com/.

Gomez-Gonzalez, M., Hernandez, J., Vera, D., Jurado, F., 2020. Optimal sizing and power schedule in pv household-prosumers for improving pv self-consumption and providing frequency containment reserve. Energy 191, 116554. URL: https://www.sciencedirect.com/science/article/pii/S0360544219322492, doi:https://doi.org/10.1016/j.energy.2019.116554.

Grosspietsch, D., Saenger, M., Girod, B., 2019. Matching decentralized energy production and local consumption: A review of renewable energy systems with conversion and storage technologies. WIREs Energy and Environment 8, e336. doi:10.1002/wene.336, arXiv:https://onlinelibrary.wiley.com/doi/pdf/10.1002/wene.336.

Hernndez, J., Sanchez-Sutil, F., Muoz-Rodrguez, F., 2019. Design criteria for the optimal sizing of a hybrid energy storage system in pv household-prosumers to maximize self-consumption and self-sufficiency. Energy 186, 115827. URL: https://www.sciencedirect.com/science/article/pii/S0360544219314999, doi:https://doi.org/10.1016/j.energy.2019.07.157.

Hernndez, J., Sanchez-Sutil, F., Muoz-Rodrguez, F., Baier, C., 2020. Optimal sizing and management strategy for pv household-prosumers with self-consumption/sufficiency enhancement and provision of frequency containment reserve. Applied Energy 277, 115529. URL: https://www.sciencedirect.com/science/article/pii/S0306261920310412, doi:https://doi.org/10.1016/j.apenergy.2020.115529.

Hou, Q., Zhang, N., Du, E., Miao, M., Peng, F., Kang, C., 2019. Probabilistic duck curve in high pv penetration power system: Concept, modeling, and empirical analysis in china. Applied Energy 242, 205 – 215.

Interreg NWE., 2019. Programme Manual v.10.

Kuboth, S., Heberle, F., König-Haagen, A., Brüggemann, D., 2019. Economic model predictive control of combined thermal and electric residential building energy systems. Applied Energy 240, 372 – 385. URL: http://www.sciencedirect.com/science/article/pii/S0306261919300996, doi:https://doi.org/10.1016/j.apenergy.2019.01.097.

Lau, E.T., Chai, K.K., Chen, Y., Loo, J., 2018. Efficient economic and resilience-based optimization for disaster recovery management of critical infrastructures. Energies 11. URL: https://www.mdpi.com/1996-1073/11/12/3418, doi:10.3390/en11123418.

Le, K.X., Huang, M.J., Wilson, C., Shah, N.N., Hewitt, N.J., 2020.

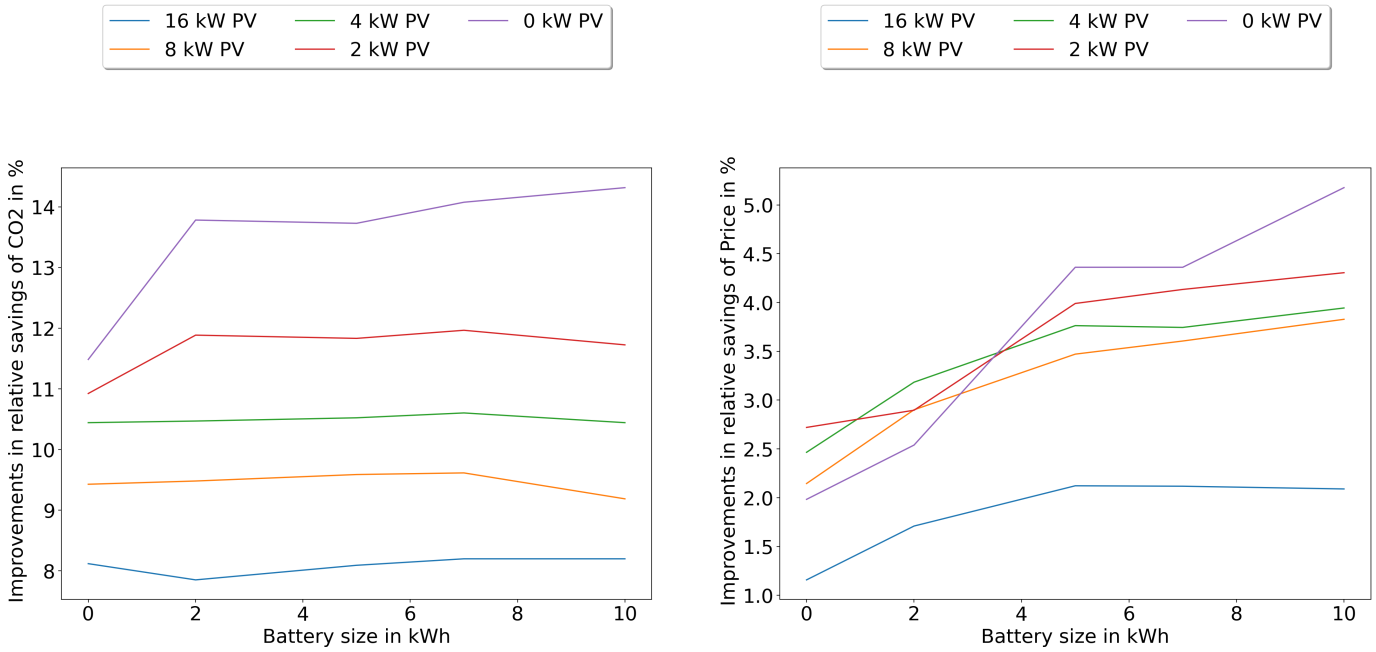

Figure 10: Comparison of RED WoLF system performance for *Case 2* in London. The left panel correspond to dependence of improvements of relative savings in CO_2 emissions on battery capacity, by the algorithm following EI signal instead of TOUT price signal. The right panel correspond to dependence of improvements of relative savings in price on battery capacity, with the algorithm following TOUT price signal instead of environmental signal. Blue, orange, green, red and purple lines are related to systems with 16 kW, 8 kW, 4 kW, 2 kW and 0 kW PV array respectively.

Tariff-based load shifting for domestic cascade heat pump with enhanced system energy efficiency and reduced wind power curtailment. Applied Energy 257, 113976.

Lichman, M., 2013. UCI machine learning repository. http://archive.ics.uci.edu/ml.

Luthander, R., Widn, J., Nilsson, D., Palm, J., 2015. Photovoltaic self-consumption in buildings: A review. Applied Energy 142, 80 – 94. URL: http://www.sciencedirect.com/science/article/pii/S0306261914012859, doi:https://doi.org/10.1016/j.apenergy.2014.12.028.

McKenna, E., McManus, M., Cooper, S., Thomson, M., 2013. Economic and environmental impact of lead-acid batteries in grid-connected domestic pv systems. Applied Energy 104, 239 – 249. URL: http://www.sciencedirect.com/science/article/pii/S0306261912008094, doi:https://doi.org/10.1016/j.apenergy.2012.11.016.

Metwaly, M.K., Teh, J., 2020. Probabilistic peak demand matching by battery energy storage alongside dynamic thermal ratings and demand response for enhanced network reliability. IEEE Access 8, 181547–181559. doi:10.1109/ACCESS.2020.3024846.

Mills, A.D., Wiser, R.H., 2015. Strategies to mitigate declines in the economic value of wind and solar at high penetration in california. Applied Energy 147, 269 – 278.

Mohamad, F., Teh, J., 2018. Impacts of energy storage system on power system reliability: A systematic review. Energies 11. URL: https://www.mdpi.com/1996-1073/11/7/1749, doi:10.3390/en11071749.

Mohamad, F., Teh, J., Lai, C.M., Chen, L.R., 2018. Development of energy storage systems for power network reliability: A review. Energies 11. URL: https://www.mdpi.com/1996-1073/11/9/2278, doi:10.3390/en11092278.

Muoz-Rodrguez, F.J., Jimnez-Castillo, G., de la Casa Hernndez, J., Aguilar Pea, J.D., 2021. A new tool to analysing photovoltaic self-consumption systems with batteries. Renewable Energy 168, 1327–1343. URL: https://www.sciencedirect.com/science/article/pii/S0960148120319984, doi:https://doi.org/10.1016/j.renene.2020.12.060.

Nacedal, J., Wright, S., 2006. Numerical optimization .

Ocotpus Energy, 2020. Octopus energy agile. URL: octopus.energy.

Ofgem, . Ofgem. URL: https://www.ofgem.gov.uk.

OpenWeather, 2019. OpenWeather. https://openweathermap.org/.

Ortiz, P., Kubler, S., ric Rondeau, Georges, J.P., Colantuono, G., Shukhobodskiy, A.A., 2021. Greenhouse gas emission reduction system in photovoltaic nanogrid with battery and thermal storage reservoirs. Journal of Cleaner Production 310, 127347. URL: https://www.sciencedirect.com/science/article/pii/S0959652621015663, doi:https://doi.org/10.1016/j.jclepro.2021.127347.

Oxford PV array, 2016. https://shkspr.mobi/blog/2014/12/a-year-of-solar-panels-open-data/.

Reda, F., Fatima, Z., 2019. Northern european nearly zero energy building concepts for apartment buildings using integrated solar technologies and dynamic occupancy profile: Focus on finland and other northern european countries. Applied Energy 237, 598 – 617. URL: http://www.sciencedirect.com/science/article/pii/S0306261919300297, doi:https://doi.org/10.1016/j.apenergy.2019.01.029.

Seo, D., Krarti, M., 2011. Hourly Solar Radiation Model Suitable for Worldwide Typical Weather File Generation. JOURNAL OF SOLAR ENERGY ENGINEERING-TRANSACTIONS OF THE ASME 133. doi:10.1115/1.4003883.

Shukhobodskiy, A.A., Colantuono, G., 2020. Red wolf: Combining a battery and thermal energy reservoirs as a hybrid storage system. Applied Energy 274. URL: www.scopus.com, doi:https://doi.org/10.1016/j.apenergy.2020.115209.

Sufyan, M., Rahim, N.A., Aman, M.M., Tan, C.K., Raihan, S.R.S., 2019. Sizing and applications of battery energy storage technologies in smart grid system: A review. Journal of Renewable and Sustainable Energy 11, 014105.

Teh, J., Lai, C.M., 2019. Reliability impacts of the dynamic thermal rating and battery energy storage systems on wind-integrated power networks. Sustainable Energy, Grids and Networks 20, 100268. URL: https://www.sciencedirect.com/science/article/pii/S2352467719304680,

doi:https://doi.org/10.1016/j.segan.2019.100268.

Telaretti, E., Graditi, G., Ippolito, M.G., Zizzo, G., 2016. Economic feasibility of stationary electrochemical storages for electric bill management applications: The italian scenario. Energy Policy 94, 126–137. URL: www.scopus.com. cited By :34.

Uddin, M., Romlie, M.F., Abdullah, M.F., Halim, S.A., Bakar, A.H.A., Kwang, T.C., 2018. A review on peak load shaving strategies. Renewable and Sustainable Energy Reviews 82, 3323 – 3332. doi:https://doi.org/10.1016/j.rser.2017.10.056.

Wagh, M., Kulkarni, V., 2018. Modeling and optimization of integration of renewable energy resources (rer) for minimum energy cost, minimum co2 emissions and sustainable development, in recent years: A review. Materials Today: Proceedings 5, 11 – 21. doi:https://doi.org/10.1016/j.matpr.2017.11.047. international Conference on Processing of Materials, Minerals and Energy (July 29th - 30th) 2016, Ongole, Andhra Pradesh, India.

Widén, J., 2014. Improved photovoltaic self-consumption with appliance scheduling in 200 single-family buildings. Applied Energy 126, 199 – 212. URL: http://www.sciencedirect.com/science/article/pii/S0306261914003419, doi:https://doi.org/10.1016/j.apenergy.2014.04.008.

Wiesheu, M., Rutei, L., Shukhobodskiy, A.A., Pogarskaia, T., Zaitcev, A., Colantuono, G., 2021. Red wolf hybrid storage system: Adaptation of algorithm and analysis of performance in residential dwellings. Renewable Energy URL: https://www.sciencedirect.com/science/article/pii/S0960148121010375, doi:https://doi.org/10.1016/j.renene.2021.07.032.

Yan, J., Yang, X., 2019. Thermal energy storage. Applied Energy 240, A1 – A6. URL: http://www.sciencedirect.com/science/article/pii/S0306261918303179, doi:https://doi.org/10.1016/j.apenergy.2018.03.001.

Zhang, N., Lu, X., McElroy, M.B., Nielsen, C.P., Chen, X., Deng, Y., Kang, C., 2016. Reducing curtailment of wind electricity in china by employing electric boilers for heat and pumped hydro for energy storage. Applied Energy 184, 987 – 994.